Supercoiled and braided DNA under tension

John F. Marko*
Center for Studies in Physics and Biology, The Rockefeller University, New York, New York 10021-6399
(Received 9 July 1996)

Double-helix DNA has a twist persistence length comparable to its bending persistence length, and thus its entropic elasticity depends on how much it is twisted. For low amounts of twist (less than about one turn per twist persistence length) there is linear elasticity for weak forces, while for large forces there is a threshold at which all chirality is expelled from the extended polymer configuration. For larger amounts of twist, plectonemic supercoiling is stabilized and there ceases to be any extension of the polymer for small forces; large forces create a mixed state of plectonemic supercoil and extended molecule. The free energy of two DNAs braided around one another is computed: to insert more than about one braid per persistence length requires expenditure of many k_BT per braid. Sufficiently tight braids wrap around themselves to form plectonemic supercoils: the force-distance behavior of braids should thus be similar to that of twisted DNA. Finally, the relevance of the thermodynamics of braiding to the disentanglement of large DNAs in living cells is discussed. [S1063-651X(97)00801-5]

PACS number(s): 87.15.−v, 36.20.Ey, 64.90.+b

I. INTRODUCTION

Double-helix DNA is a stiff polymer. In a room temperature aqueous solution, the tangent vector to the molecule is reoriented by thermal bends roughly once every thermal bending persistence length, $A=50$ nm [1]. Due to its structure—two single strands wrapped around one another—the double helix also has twist elasticity. Thermal fluctuations cause random twisting by about one radian every twisting persistence length of $C=75$ nm [2,3]. This paper discusses how the entropic elasticity of DNA, or any wormlike chain with twist rigidity, is affected by twisting.

To separate the ends of a DNA by half of its total contour length requires a tension of about $k_BT/A\approx 0.08$ pN; at this point, applied tension starts to overwhelm thermally excited bending. Measurement of this entropic elasticity for single DNA molecules of contour length $L\approx 10$ to 100 μm (many persistence lengths) is now an experimental reality [4,5]. Such experiments exploit the specificity of DNA's base pairing to make single-stranded attachments of DNAs to microscope slides and magnetic beads [Fig. 1(a)]. However, the molecule can swivel around the single bonds in single-stranded attachments, eliminating the possibility of applying twist to the molecule. Both strands must be anchored at both ends of the molecule in order to study its elasticity as a function of twisting [Fig. 1(b)].

If the anchoring points are on inpenetrable walls, the topological linkage number Lk of the double helix is fixed. The physics problem relevant to the elasticity of twisted DNA is therefore the statistical mechanics of the double helix under tension subject to the constraint of fixed Lk. In general a DNA with constrained Lk is referred to as ''supercoiled.'' The shape of a supercoiled DNA becomes highly perturbed from a random walk when Lk is changed from its equilibrium value by more than one link per thermal twist persistence length C. Since the double helix twists through one radian every 0.6 nm of contour length, this point is reached when Lk is perturbed by about 1% [6].

Given sufficient twisting stress, there occurs a buckling and wrapping of the double helix around itself in the same way that a telephone cord wraps around itself if the receiver is twisted a few times before it is hung up [Fig. 2(a)]. This ''plectonemic supercoiling'' achieves a reduction in twisting energy at the expense of some bending energy and confinement entropy. Plectonemic interwinding does not allow the molecule to traverse distance and will be destabilized by applied tension, while an ''extended supercoil'' state should be stabilized by tension. This was previously discussed [6], and the aim of Sec. II is to give a more complete and analytical account of the theory, including comparison with experiments of Strick *et al.* [7]. In addition to entropic elasticity implying plectonemic and extended supercoiling, experiment indicates, in agreement with the prediction, that the double helix undergoes abrupt structural transitions for forces ≈ 1 pN if Lk is perturbed by $\approx 5\%$. Without twisting stress, such structural transitions occur for much larger applied forces ≈ 50 pN [8,9].

One can imagine braiding two polymers together so that their linkage number is fixed. This is analogous to the

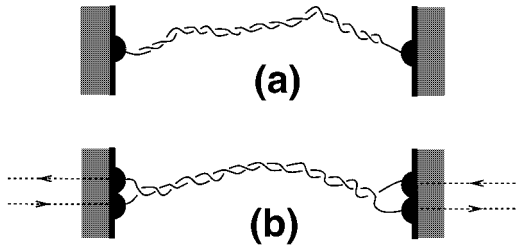

FIG. 1. Double-stranded DNA with (a) single-strand attachments and (b) double-strand attachments to two parallel ''walls.'' The linkage of the two strands is held fixed only in (b); Lk may be defined by continuation of the strands so that they close at infinity (dashed lines).

*Present address: Department of Physics, The University of Illinois at Chicago, 845 West Taylor St., Chicago, IL 60607-7059.

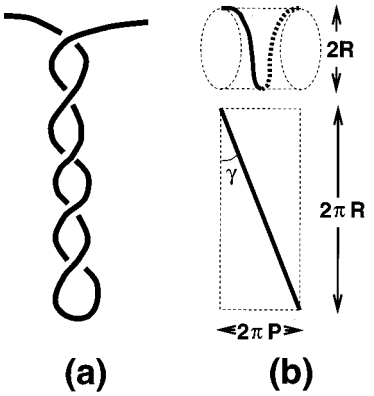

FIG. 2. (a) Plectonemic supercoil (heavy line represents double-stranded DNA); (b) a right helix is described by its radius R and pitch P; the helical repeat is $2\pi P$ and the contour length of one turn is $2\pi\ell = 2\pi(R^2+P^2)^{1/2}$.

fixed-Lk situation described above, where single strands are replaced with double helicies. Strick *et al.* [7] have achieved this by micromanipulation of two DNAs (just one strand of each double helix was tethered so that neither of the double-helix linkages was held fixed; one could imagine doing this with any polymer as the double-helix twist rigidity plays no role). Circular DNAs are often toroidally linked after their replication in cells, and may also be considered to be braids [10,11]. Section III discusses the statistical mechanics of braided DNAs: the free energy as a function of linkage for simple braids is computed: a novel type of ''phase separation'' of the braiding is predicted. Highly twisted braids are found to form plectonemic supercoils analogous to those formed by DNA. Also, the entropic elasticity of braids is discussed. Finally, the biophysical implications of these problems are discussed, notably the possible role of thermodynamics in the removal of braidlike entanglements, a process that must occur in cells to separate long DNAs after their replication [12].

II. STRETCHING SUPERCOILED DNA

Consider a double-stranded DNA (dsDNA) of length L, pulled to an extension z, attached to walls that may be rotated to twist the molecule (throughout this paper L is the total contour length of the *relaxed* DNA in question: under tensions >20 pN the contour length can increase via distortion of the double helix [8,9]). The long-chain limit $L/A\to\infty$ is assumed; the recent experiments of Strick *et al.* [7] have $L/A\approx 320$. Unperturbed dsDNA adopts a helix repeat of $h\approx 3.5$ nm containing 10.5 base pairs (bp), with an equilibrium twist rate of $\omega_0 = 2\pi/h \approx 1.8\ \mathrm{nm}^{-1}$. A relaxed double helix thus has a linkage of about $\mathrm{Lk}_0 \equiv L/h$.

A. Linking number of a stretched DNA

For a *closed* dsDNA, the linking number of the two closed single strands $\mathbf{r}_+$ and $\mathbf{r}_-$ is given by Gauss' formula

$$\mathrm{Lk} = \oint \oint \frac{d\mathbf{r}_+ \times d\mathbf{r}_- \cdot (\mathbf{r}_+ - \mathbf{r}_-)}{4\pi |\mathbf{r}_+ - \mathbf{r}_-|^3}. \tag{1}$$

The two strands $\mathbf{r}_\pm$ are held closely together by hydrogen bonds to form a cylindrical structure with a diameter of about 2 nm. Given that the DNA diameter is narrow compared to typical bends, it is useful to chop Eq. (1) into two geometrical quantities [13]

$$\mathrm{Lk} = \mathrm{Tw} + \mathrm{Wr}. \tag{2}$$

The ''writhe'' Wr is Eq. (1) with $\mathbf{r}_+$ and $\mathbf{r}_-$ *each* replaced by the central axis $\mathbf{r}$ (the middle of the cylindrical dsDNA); the nonlocal Wr measures the contribution of crossings of the molecule over itself to Lk.

The ''twist'' Tw is the total local circulation of the strands around the double-helix central axis [13]

$$\mathrm{Tw} = \frac{1}{2\pi} \oint d\mathbf{u} \cdot \mathbf{t} \times \mathbf{u}, \tag{3}$$

where $\mathbf{t}$ is the unit tangent to the central axis, and $\mathbf{u}$ is a unit vector perpendicular to $\mathbf{t}$ pointing from the central axis towards one of the strands. It is useful to consider the excess twist $\Delta\mathrm{Tw} = \mathrm{Tw} - \mathrm{Lk}_0$, and the excess linkage $\Delta\mathrm{Lk} = \mathrm{Lk} - \mathrm{Lk}_0$, with respect to the relaxed double helix for which $\mathrm{Tw} = \mathrm{Lk} = \mathrm{Lk}_0$.

Using arc length s to parametrize $\mathbf{r}(s)$, the excess twist is

$$\Delta\mathrm{Tw} = \int_0^L \frac{ds}{2\pi} (\mathbf{t} \times \mathbf{u} \cdot \partial_s \mathbf{u} - \omega_0). \tag{4}$$

Assuming an elastic rod model for small distortions of ds-DNA [6,14], the leading term in the twist energy per length of DNA is the integrand of Eq. (4) squared, times $C/2$. Keeping only this contribution, fluctuations of the twist can be integrated (the fixed-Lk constraint affects only total twist), leaving

$$\frac{E_{\mathrm{twist}}}{k_B T L} = \frac{C}{2} \left(\frac{2\pi \Delta\mathrm{Tw}}{L} \right)^2 = \frac{2\pi^2 C}{L^2} (\Delta\mathrm{Lk} - \mathrm{Wr})^2. \tag{5}$$

The final term is the twist energy per length at fixed Lk, given the Wr of the configuration. It can be seen that the twist energy can be reduced if $\mathrm{Wr} \approx \Delta\mathrm{Lk}$: the constraint of fixed Lk generates a long-ranged interaction which drives supercoiling.

For a *linear* DNA attached to two walls, Lk is defined by counting the number of full twists that must be made of one wall to unlink the intervening DNA strands; ΔLk is simply the number of twists of the wall needed to relax the molecule. To calculate Lk for an arbitrary conformation using Eqs. (1) and (2), one must construct an imaginary closure path outside the walls. It is convenient to suppose that there is zero twist along the closure [dashed lines of Fig. 1(b)], since then only the Wr of the closure contributes to Lk. If the closure path is chosen to go out to infinity from the attachment points of the molecule to the wall as straight lines normal to the walls, the contribution of the closure to Wr may be shown to grow with L no faster than $\sim[\ln(L/A)]^{1/2}$ (the closure contribution can be shown to be smaller than the linkage of a straight rod with a random coil for which there are exact results for Gaussian polymers [15] and for self-avoiding chains [16]). Since ΔLk scales with L, for $L \gg A$,

the contribution to Wr of the closure may be ignored, and Lk may be computed using only the Tw and Wr of the linear DNA.

In the experiments of Strick *et al.* [7], one end of the molecule is attached to a bead, and therefore one of the ''walls'' of Fig. 1(b) is effectively only a few micrometers high. Therefore it is possible for the DNA contour to thermally wander over the bead, and thus pass through the ficticious closure path. This, of course, changes the value of Lk by ± 2, and some care should be taken to use a large enough bead, and to keep sufficient tension on the DNA, such that the linkage does not ''leak away'' by a series of such events (no such leakage occurred in the experiments of Strick *et al.*). The kinetics of this Lk relaxation would be interesting to study as a function of tension; such an experiment comprises an artificial ''topoisomerase'' where the molecule is able to pass through a gap in its own contour, with a change of linkage number of ± 2 with each passage.

B. Free energy of stretched twisted DNA

For a long DNA, linkage is conveniently described using the intensive excess linking number density $\sigma \equiv \Delta \mathrm{Lk}/\mathrm{Lk}_0$. Consider a mixed state with a fraction x_s of the molecule extended, and $1-x_s$ plectonemically supercoiled. Each plectonemic region is geometrically nearly a closed loop of DNA (imagine pinching off a closed plectoneme at each junction point of extended and plectonemic DNA), thus linkage densities σ_s and σ_p may be defined for the extended and plectonemic regions, respectively, subject to the constraint $\sigma = x_s \sigma_s + (1-x_s)\sigma_p$.

Given total extension z the free energy per length is [6]

$$\mathcal{F}(\sigma, z/L) = \min_{x_s, \sigma_s} [x_s \mathcal{F}_s(\sigma_s, y) + (1-x_s)\mathcal{F}_p(\sigma_p)]. \quad (6)$$

The plectoneme free energy per length $\mathcal{F}_p$ depends only on σ_p, while the extended free energy per length $\mathcal{F}_s$ depends on σ_s and extension as a fraction of the length of DNA in the extended region, $y \equiv z/(x_s L)$. The force f needed to attain extension z is

$$f = \frac{\partial \mathcal{F}}{\partial z/L}. \quad (7)$$

Note that the ''pure'' plectoneme and extended states have very different elastic behaviors. Plectonemic domains are inextensible by definition since they are closed loops. The extended ''solenoid'' regions by contrast may undergo random bends at length scales large compared to their superhelix repeat, and therefore should display polymerlike linear elasticity at low forces. Thus the final ''mixed'' state can display either of these behaviors for low forces, depending on whether it is fully plectoneme, or a partially or fully extended solenoid.

C. Plectoneme free energy

The plectoneme free energy was studied in detail previously [6]. The equilibrium superhelical pitch P [the superhelical repeat length is $2\pi P$, see Fig. 2(b)] and radius R are determined variationally from

$$\frac{\mathcal{F}_p(\sigma)}{k_B T} = \min_{R,P} \left[\frac{A}{2} \frac{R^2}{(R^2+P^2)^2} + \frac{C}{2} \left(\sigma \omega_0 \pm 2\pi \frac{P}{R^2+P^2} \right)^2 + A^{-1/3} (\pi P)^{-2/3} + A^{-1/3} R^{-2/3} + w(R) + w(\pi P) \right]. \quad (8)$$

The first two terms give the bending and twisting energy, the next two terms account for the entropy lost by confining the DNA into the superhelix, and the last two terms account for direct electrostatic repulsion of the helicies juxtaposed in the supercoil. The bending energy is $A/2$ times the axis curvature squared. The twisting energy is of the form (5), using the Wr per length for a regular plectoneme, $2\pi \mathrm{Wr}/L = \mp P/(P^2+R^2)$; upper and lower signs are for right- and left-handed plectonemes, respectively. The twist energy is minimized, for $\sigma > 0$, by a left-handed plectoneme; below, this case is considered ($\sigma < 0$ is obtained simply by reversing the handedness).

The persistence lengths are taken to be $A = 50$ nm, and $C = 75$ nm. The energy per length in $k_B T$ units of electrostatic interactions is $w(x) = \ell_B \nu^2 K_0(2x/\lambda_D)$, where the Bjerrum length $\ell_B = e^2/(\epsilon k_B T)$ is 0.7 nm in water at 300 K, $\lambda_D = (0.3\ \mathrm{nm})/M^{1/2}$ for univalent salt at molarity M, and where ν is an effective charge which is 8.4 nm^{-1} for 0.15 M NaCl, and 2.5 nm^{-1} for 0.01 M NaCl, the two cases considered here [17].

The plectoneme free energy that results from this free energy has the following properties. If $|\sigma|$ is below a critical linking number $\sigma^* \approx 0.02$, there is no minimum of the free energy with R and P finite: the confinement entropy cost overwhelms the energy gain of supercoiling. For $|\sigma| > \sigma^*$ plectonemic supercoils are stable, and their free energy increases with $|\sigma|$ much slower than that of unsupercoiled DNA. This is because cancellation of ΔLk by Wr, and therefore reduction of the twist energy (5), can be achieved with almost no bending energy cost for the plectoneme. Figure 3 shows the free energy per length of the plectonemic state obtained from Eq. (8), for electrostatic interactions appropriate for 0.14 M and 0.01 M univalent salt concentration.

The plectoneme free energy initially increases nearly linearly for $|\sigma| > |\sigma^*|$ due to near-total cancellation of linkage by writhe. However, once the helicies are squashed together to the point where the electrostatic interactions begin to dominate, the twist energy and, therefore, the free energy, starts to increase quadratically with $|\sigma|$. For 0.01 M NaCl, this change from linear to quadratic dependence is at about $|\sigma| = 0.04$; for 0.15 M NaCl, the shorter range of the electrostatic interaction delays this to about $|\sigma| = 0.07$ (see Fig. 3).

This range of $|\sigma|$ where $\mathcal{F}_p$ increases nearly linearly suggests that one might expect ''phase coexistence'' of domains of random coil and supercoil. There exist electron-microscope pictures suggestive of coexistence of supercoiled and disordered, loosely coiled regions on a single circular DNA [18], but this interpretation must be tempered by the expectation of strong fluctuations for this one-dimensional system. Instead of robust phase coexistence of high-σ and low-σ states, large fluctuations in the structure of supercoils can be expected in the regime where $\mathcal{F}_p$ grows linearly with $|\sigma|$. However, once the DNA is put under tension, extension

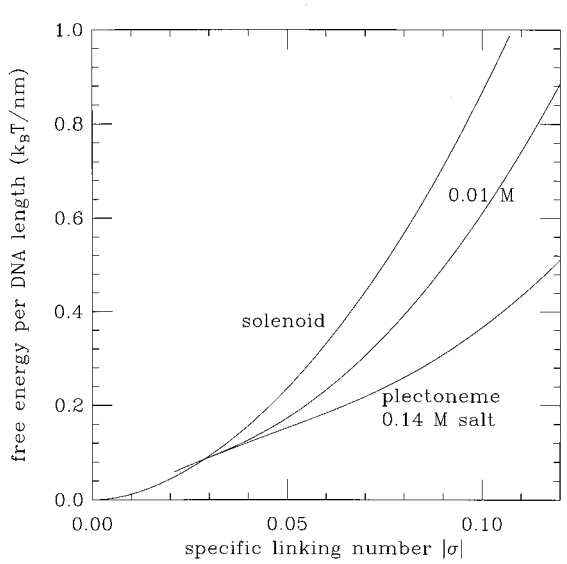

FIG. 3. Free energy per length of plectonemic and solenoidal supercoiled DNA as a function of linking number, for $A=50$ nm and $C=75$ nm. For 0.01 M and 0.14 M univalent salt, the plectonemic state becomes stable for $|\sigma|\approx 0.02$. In the 0.01 M case, weaker screening of electrostatic interactions leads to an increase in the free energy relative to the 0.14 M case. The solenoid state (Sec. II D) has a lower free energy than the plectoneme (Sec. II C) for $|\sigma|<0.029$.

by force will make unsupercoiled-supercoiled phase coexistence more robust, since a large free energy cost will be established for fluctuations of the partitioning.

D. Stretched solenoid free energy

As a model for an extended supercoil, consider a solenoid of mean radius R and pitch P [Fig. 2(b)]. One radian of superhelix contains a contour length $\ell=\sqrt{R^2+P^2}$. The sine of the superhelix opening angle [Fig. 2(b)] is $\sin\gamma\equiv P/\ell$; the case $\sin\gamma=1$ is a straight line ($R=0$), while $\sin\gamma=0$ is a circle ($P=0$). The parameters ℓ and $\sin\gamma$ are more convenient than R and P for what follows.

For large forces ($f\gg k_BT/A$), the free energy per length for the solenoid in fixed-force ensemble is of the form [6]

$$\frac{\mathcal{G}(\sigma,f)}{k_BT}=\frac{A\cos^2\gamma}{2\ell^2}+\frac{C}{2}\left(\sigma\omega_0\mp\frac{1-\sin\gamma}{\ell}\right)^2-\frac{fs}{k_BT}+\left(\frac{f}{k_BTA\sin\gamma}\right)^{1/2}. \tag{9}$$

The solenoid writhe per length, $2\pi \mathrm{Wr}/L=\pm(1-\sin\gamma)/\ell$, appears in the twist energy; the bending energy is as in Eq. (8). The twist energy is minimized for $\sigma>0$ by a right-handed solenoid: the formulas below assume this case. The final fluctuation term is the large-force limit of a more complicated expression obtained from a detailed calculation [6]; use of this limit allows the solenoid state to be treated analytically.

Minimizing $\mathcal{G}$ with respect to ℓ gives $\ell=[(1+\sin\gamma)A+(1-\sin\gamma)C]/X$, where $X\equiv C\sigma\omega_0$ measures excess linkage per twist persistence length. Minimizing $\mathcal{G}$ with respect to $\sin\gamma$ gives $A/\ell^2=f/k_BT+\sqrt{f/(4k_BTA\sin^3\gamma)}$, which for large forces is approximately $\ell=\sqrt{k_BTA/f}$. Thus ℓ is the correlation length for the fluctuations in the high-force limit, as occurred for plectonemic supercoiling [6]. Now the equilibrium value of $\sin\gamma$ may be solved for

$$\sin\gamma=\begin{cases}\dfrac{C+A-X\ell}{C-A}, & f\leqslant f^*\\ 1, & f\geqslant f^*,\end{cases} \tag{10}$$

where $f^*\equiv k_BTX^2/(4A)$, and where $C>A$ is assumed. Note the boundary minimum ($\sin\gamma=1$) that appears for sufficiently large forces due to the fact that $0\leqslant\sin\gamma\leqslant 1$ (this effect was observed in the previously published numerical treatment of the solenoid state [6]). High enough forces ($>f^*$) thus completely expel the writhe. Note that f^* is in the regime where the calculation is viable ($f^*\gg k_BT/A$) only when $X>1$, and also that if $C<A$, $\sin\gamma=1$ for all forces.

The free energy of the solenoid for $f\gg k_BT/A$ is therefore

$$\mathcal{G}=\begin{cases}\left(1+\dfrac{2A}{C-A}X\right)\sqrt{k_BTf/A}-\left(1+\dfrac{2A}{C-A}\right)f-k_BT\dfrac{A}{2C}\dfrac{X^2}{C-A}, & f\leqslant f^*\\ \sqrt{k_BTf/A}-f+k_BT\dfrac{X^2}{2C}, & f\geqslant f^*.\end{cases} \tag{11}$$

The extension (as a fraction of molecule length) is $y=-\partial\mathcal{G}/\partial f$, or

$$y=\begin{cases}1+\dfrac{2A}{C-A}-\left(1+\dfrac{2A}{C-A}X\right)\Big/\sqrt{4Af/k_BT}, & f\leqslant f^*\\ 1-1/\sqrt{4Af/k_BT}, & f\geqslant f^*.\end{cases} \tag{12}$$

Inversion of Eq. (12) gives force as a function of extension

$$\frac{fA}{k_BT}=\begin{cases}\dfrac{1}{4}\left(1+\dfrac{2A}{C-A}X\right)^2\left(1+\dfrac{2A}{C-A}-y\right)^{-2}, & y\leqslant 1-\dfrac{1}{X}\\ \dfrac{1}{4}(1-y)^{-2}, & y\geqslant 1-\dfrac{1}{X}.\end{cases} \tag{13}$$

To construct a reasonable low-force, low-extension limit (this regime was not previously described [6]) with linear

elasticity at low force, add terms $ay+b$ to the force vs extension, where a and b are different for $y \geqslant 1-1/X$ and $\leqslant 1-1/X$. For $y \geqslant 1-1/X$, $a+by=y-1/4$, since the force distance must be the $\sigma=0$ result [19] if the linking number is expelled from the writhe. Requiring continuity at $y=1-1/X$, and requiring the force to vanish as $y \to 0$ fixes the force law (the assumption of linear elasticity at low forces follows after noting that the extended solenoid state can undergo random-walk fluctuations at length scales $\gg \ell$)

$$\frac{fA}{k_BT}=\begin{cases} \dfrac{1}{4}\dfrac{\left(1+\dfrac{2A}{C-A}X\right)^2}{\left(1+\dfrac{2A}{C-A}-y\right)^2}-\dfrac{1}{4}\left[\dfrac{\left(1+\dfrac{2A}{C-A}X\right)^2}{\left(1+\dfrac{2A}{C-A}\right)^2}-1\right]\left[1-\dfrac{y}{1-1/X}\right]+y-\dfrac{1}{4}, & y \leqslant 1-\dfrac{1}{X} \\ \dfrac{1}{4}(1-y)^{-2}+y-\dfrac{1}{4}, & y \geqslant 1-\dfrac{1}{X} \end{cases} . \tag{14}$$

This force vs extension for a variety of $|\sigma|$ values is shown in Fig. 4, for $A=50$ nm and $C=75$ nm. For $X<1$, or $|\sigma|<0.01$, the force is increased from the $\sigma=0$ case only slightly, at small extensions. For larger $|\sigma|$, more force is required to obtain a given extension over most of the extension range: only for large forces $f>f^*$ does the force law revert to the $\sigma=0$ case.

The free energy is obtained by integration of Eq. (14):

$$\frac{\mathcal{F}_s(\sigma,y)}{k_BT/A}=\begin{cases} \dfrac{1}{4}\dfrac{\left(1+\dfrac{2A}{C-A}X\right)^2}{1+\dfrac{2A}{C-A}-y}+\dfrac{1}{8}\left[\dfrac{\left(1+\dfrac{2A}{C-A}X\right)^2}{\left(1+\dfrac{2A}{C-A}\right)^2}-1\right]\left[\dfrac{y^2}{1-\dfrac{1}{X}}-2y-\dfrac{1}{X}+1\right] \\ \qquad +\dfrac{y^2}{2}-\dfrac{y}{4}-\dfrac{1}{4}-\dfrac{A^2}{2C(C-A)}X^2, \quad y \leqslant 1-\dfrac{1}{X} \\ \dfrac{1}{4}(1-y)^{-1}+\dfrac{1}{2}y^2-\dfrac{1}{4}y-\dfrac{1}{4}+\dfrac{A}{2C}X^2, \quad y \geqslant 1-\dfrac{1}{X} \end{cases} \tag{15}$$

where the constant of integration has been set by recognizing that for $y \geqslant 1-1/X$ the free energy should be that of a nonchiral chain plus the twist free energy per length $X^2/2C$, and by requiring continuity of the free energy to the regime $y \leqslant 1-1/X$.

Setting $y=0$ in Eq. (15) gives a model for the random-coil to solenoidal-supercoil transition: for $X<1$, all link is in twist, while for $X>1$ some link is transferred to writhe. The free energy per length of this random coil/solenoid state $\mathcal{F}_s(\sigma,0)$ is shown in Fig. 3; for large X it grows as

$$\frac{\mathcal{F}_s(\sigma,0)}{k_BT} \approx \frac{A(A+2C)}{(A+C)^2}\frac{X^2}{2C}. \tag{16}$$

This is slightly less than the ''unscreened'' twisting energy per length $X^2/2C$, and just slightly higher than the solenoid supercoil free energy calculated previously [6], which had the scaling limit $[A/(A+C)][X^2/(2C)]$. One should also note that the plectoneme free energy $\mathcal{F}_p(\sigma)$ and the unstretched solenoid free energy $\mathcal{F}_s(\sigma,y=0)$ are very nearly equal at the transition point σ^*. Thus, the unstretched solenoid state is a reasonable description of a supercoiled DNA with $|\sigma|<\sigma^*$.

E. Stress-induced denaturation of stretched twisted DNA

The descriptions of the plectoneme and the solenoid states assumed harmonic bending and twisting energies. These approximations can be expected to break down when the energy associated with twisting or bending becomes comparable with the cohesive free energy per length of dsDNA of $\approx 10 k_BT$/nm at 300 K (roughly 3 k_BT per base pair [19]): this is a force of about 40 pN. DNA should be deformed by forces larger than this, and recently it was observed that the double helix gradually stretches for forces above about 20 pN, and then abruptly stretches to about twice its relaxed contour length at 65 pN [8,9]. This length increase is consistent with straightening out of the normally helical phosphate-sugar backbones. Such drastic changes of double helix structure will be referred to here as ''denaturation.''

The structure of tension-denatured DNA is poorly understood. Experiments indicate that the work done when the helicies are straightened is significantly less than the free energy necessary to separate and extend the two strands, suggesting that the two strands of the stretched molecule are still base paired (integration of the force up to the end of the overstretching ''plateau'' in Fig. 2 of Ref. [9] yields a total work done of 13 k_BT/nm; this is less than the 10 k_BT/nm helix-coil free energy difference [19] plus the 12 k_BT/nm stretching free energy of the two single strands, which may

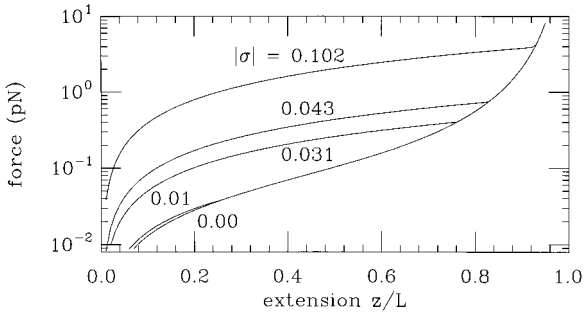

FIG. 4. Force vs extension of the extended supercoil state, for $A=50$ nm and $C=75$ nm. For $|\sigma|<0.01$, the behavior is very close to that of $\sigma=0$ (lowest curve); as $|\sigma|$ is increased, progressively more force is required to obtain a given extension.

be estimated from Fig. 6 of Ref. [9]). This is consistent with molecular modeling results [8].

The tension necessary to denature DNA will come down if the molecule is twisted. For $|\sigma|<0.02$ the stress associated with twisting is $\approx k_BTC\omega_0^2\sigma$ or $\approx 4k_BT$/nm (with respect to the strain variable σ which locally jumps by order unity during denaturation). Twisting of $|\sigma|\approx 0.02$ should therefore lead to a few pN reduction in the tension necessary to totally overstretch a DNA.

For $|\sigma|>0.02$ supercoiling occurs, raising the question of whether denaturation will occur in the extended region of the DNA, or in the plectonemic region of the DNA. For the twist energy assumed in this paper Eq. (5), the mean twist is the same in the two regions. To completely understand where the denaturation will occur requires a detailed model of how twisting is coupled to stretching of the molecule, including nonlinearities that will generate transitions to denatured states. This most general approach is not followed in this paper. Instead, the simplifying assumption is made that denaturation occurs in ''bubbles'' which do not contribute to chain extension; this is equivalent to assuming denaturation occurs in the plectonemic region of the chain.

For higher forces, elasticity very similar to that of untwisted DNA should be observed, since once the initial denaturation occurs, the linking number will have been relaxed. Denaturation of the remainder of the chain (as would be diagnosed by a factor-of-2 change in apparent length) should occur for high forces on the order of 65 pN. Thus there will be two force plateaus, the first involving a jump of extension to close to the *B*-form length, and the second making a further jump to the extended-form length (roughly twice the *B*-form length).

To describe denaturation in the plectonemic region, only a slight modification of the plectoneme free energy is needed. Assuming that denaturation costs a certain free energy per length Δ, then the free energy of a plectoneme that has undergone denaturation of a fraction x of its length is

$$\mathcal{F}_p(\sigma)=(1-x)\mathcal{F}_{p,0}(\sigma_0)+x\Delta, \tag{17}$$

where σ_0 is the linking number in the undenatured plectoneme region, and where the free energy without denaturation Eq. (8), is denoted $\mathcal{F}_{p,0}$. The linking number of the denatured state is assumed to be fixed at σ_D: thus Eq. (17) is minimized subject to the constraint $\sigma=(1-x)\sigma_0+x\sigma_D$. The result is

$$\mathcal{F}_p(\sigma)=\begin{cases}\mathcal{F}_{p,0}(\sigma), & |\sigma|<|\sigma_d|\\ \mathcal{F}_{p,0}(\sigma_d)+\mathcal{F}'_p(\sigma_d)|\sigma-\sigma_d|, & |\sigma|>|\sigma_d|\end{cases}$$

$$x=\begin{cases}0, & |\sigma|<|\sigma_d|\\ (\sigma_p-\sigma_d)/(\sigma_D-\sigma_d), & |\sigma|>|\sigma_d|,\end{cases} \tag{18}$$

where the denaturation point σ_d is defined by the equation

$$\mathcal{F}'_{p,0}(\sigma_d)=\frac{\Delta-\mathcal{F}_{p,0}(\sigma_d)}{\sigma_D-\sigma_d}. \tag{19}$$

This is phase coexistence of plectonemic and denatured DNA.

Above, denaturation was characterized by the two parameters Δ and σ_D; alternatively, it is convenient to use σ_d and σ_D, specific linking numbers of the ''coexisting'' plectonemic and denatured ''phases.'' The free energy $\mathcal{F}_p$ is constructed from $\mathcal{F}_{p,0}$ by just extending it linearly from σ_d to σ_D. The free energy of the denatured state follows from Eq. (18) as

$$\Delta=\mathcal{F}_p(\sigma_d)+(\sigma_D-\sigma_d)\mathcal{F}'_p(\sigma_d). \tag{20}$$

F. Results and comparison with experiments

Recently, Strick *et al.* [7] have measured the extension as a function of applied force and linking number, for a long ($\approx$50 000 bp=50 kb=17 μm) DNA, in buffer with univalent ions at a concentration of 0.01 M. If one assumes $A=50$ nm and $C=75$ nm, the denaturation parameters σ_d and σ_D remain to be set by comparison with experiment.

Experiments were done for positive excess linkages $\sigma=0.0$, 0.01, 0.031, 0.043, and 0.102 [Fig. 5(a)]. The $\sigma=0$ experimental result agrees quantitatively with previous measurements of the entropic elasticity of untwisted DNA. Theoretical force-distance curves are shown in Fig. 6(a); the choice $\sigma_d=0.12$ and $\sigma_D=1.0$ generates a prominent plateau for $\sigma=0.102$. These denaturation parameters correspond to a free energy of the denatured state $\Delta=14.5\ k_BT$/nm. This is similar to the amount of work that must be done to separate the strands of dsDNA [19]; the value $\sigma_D=1$ corresponds to a helix repeat of 5 bp instead of the usual 10. The reader is cautioned that no other evidence exists for such an overtwisted state of the double helix; however, no other experiments have been done for such large positive σ.

For $\sigma\leqslant 0.043$, the theoretical and experimental force-distance curves are both smooth, indicating no denaturation. For $\sigma=0.031$ and 0.043, theory and experiment agree that the force is much higher than that of $\sigma=0$ over most of the extension range; theory indicates that the plectonemic state is in coexistence with extended DNA all the way up to the point where the force curve collides with the $\sigma=0$ curve. For the $\sigma=0.043$ case, the finite force at which extension starts to occur is close to that observed experimentally; the existence of a finite force at zero extension is the first evi-

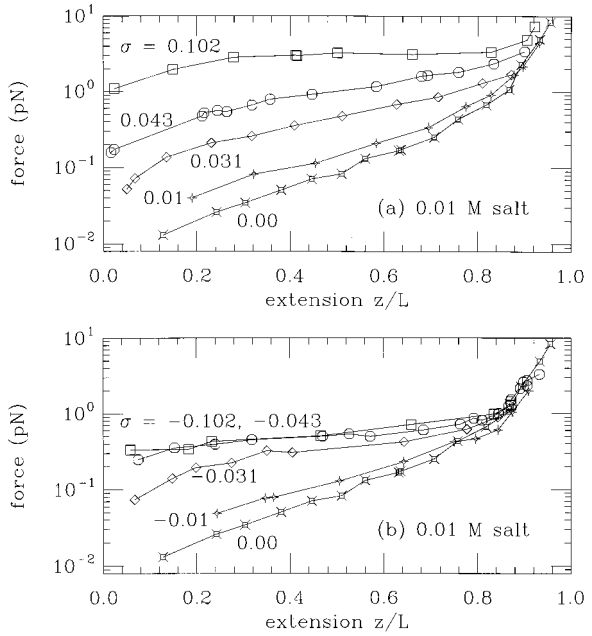

FIG. 5. Experimental force vs extension data of Strick *et al.* [7] for twisted dsDNA. For specific linking $\sigma=0$, the data follow the elasticity law for the wormlike chain, while for $|\sigma|>0$, force progressively shifts up for a given extension. (a) Overwound DNA. The case $\sigma=0.01$ is only slightly shifted above the $\sigma=0$ curve; the $\sigma=0.031$ data are much higher in comparison. For $\sigma\geqslant 0.043$ force approaches a finite value at zero extension. In the highly twisted case $\sigma=0.102$, there is a prominent force plateau at about 3 pN, possibly indicating a structural transition or denaturation of the DNA. (b) Underwound DNA. For $\sigma=-0.01$ and -0.031, the data are similar to those for overwound DNA, but a large difference is seen for $\sigma=0.043$, where a force plateau appears at about 0.6 pN.

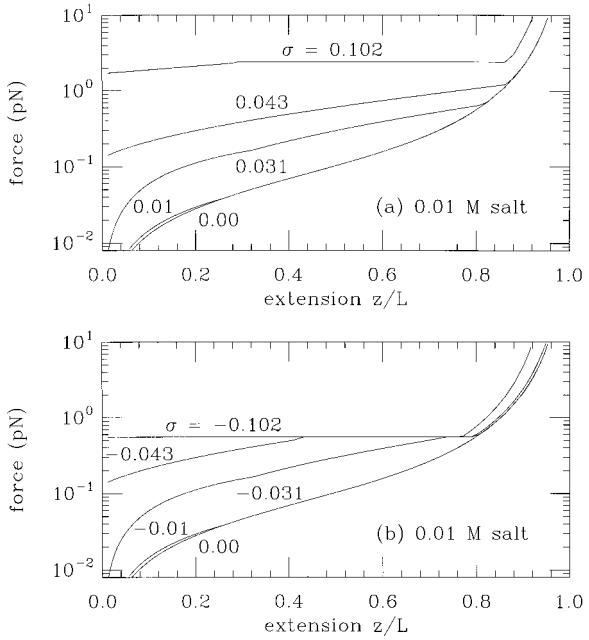

FIG. 6. Theoretical force vs extension for twisted DNA, including coexistence of plectonemic, extended, and denatured states. All curves are for 0.01 M univalent salt, $A=50$ nm, $C=75$ nm. (a) Overwound DNA ($\sigma_d=0.12$, $\sigma_D=1.0$): For $\sigma<0.01$, the force is nearly the same as the $\sigma=0$ curve. For $\sigma\geqslant 0.031$, a large shift in force is seen, and for $\sigma=0.043$, force approaches a finite value at zero extension, reflecting that the molecule is fully supercoiled. For $\sigma=0.102$, a force plateau at 2 pN occurs, reflecting the appearance of denatured bubbles along the molecule. (b) Underwound DNA ($\sigma_d=-0.06$, $\sigma_D=-2.0$): Results for $\sigma=-0.01$ and -0.031 are the same as in the overwound case, but for $\sigma=-0.043$ denaturation (force plateau) occurs at 0.6 pN. For $\sigma=-0.102$ plectonemic DNA is denatured, so the force plateau extends down to zero extension in that case.

dence that plectonemic supercoiling can be considered as a thermodynamic ''phase.'' For $\sigma=0.031$, experimental and theoretical forces both dip down near zero extension: in the case of theory, this is because at zero tension, theory indicates an equilibrium state which is roughly half plectoneme and half solenoid.

For $\sigma<0$, the double helix is being unwound, and therefore should denature at lower forces. Experimental data for 0.01 M univalent salt shown in Fig. 5(b) bear this out: $\sigma=-0.043$ and 0.102 data indicate a force plateau at about 0.5 pN, significantly below the force plateau seen for $\sigma>0$. At the same time, it should be noted that for $|\sigma|\leqslant 0.031$ and forces <0.5 pN, the experimental data are quite similar to those for $\sigma>0$, suggesting that there is a range of σ where the DNA elasticity is reasonably harmonic (i.e., that $A=50$ nm and $C=75$ nm are appropriate for $\sigma>0$ and $\sigma<0$). Therefore, the differences between overwound and underwound DNA might be captured simply by the use of different denaturation parameters in the two cases.

The DNA in supercoiled plasmids is known to form ''noncanonical structures'' (i.e., non-*B*-DNA) for $\sigma\leqslant -0.06$, thus $\sigma_d=-0.06$ is plausible for underwound DNA [21]. One of those noncanonical forms is *Z* DNA, a dsDNA state with one left-handed turn every 10 bp, thus $\sigma_D=-2$ is plausible. These parameters give a denatured state with free energy $\Delta=13.7k_BT$/nm above that of unperturbed dsDNA (again on the order of the free energy difference between double helix and separated strands). Taking these parameters gives the force-distance curves shown in Fig. 6(b). For $\sigma=-0.01$ and over almost all of the range of $\sigma=0.031$, theory gives the same result as for $\sigma=0.01$ and 0.031. For $\sigma=-0.043$, theory indicates that the force at zero extension is finite, and it starts out following the same curve as for $\sigma=0.043$; however, the lower $|\sigma|$ required for denaturation causes a force plateau at about 0.6 pN. For $\sigma=-0.102$, the DNA is partially denatured even without applied tension, thus the theoretical force plateau extends all the way down to zero extension in this case; as a result, the theoretical $\sigma=-0.102$ curve is well below that for $\sigma=0.102$ for low extensions.

The experimental results suggest three regimes: (a) for $|\sigma|\leqslant 0.01$ nearly the same elasticity as untwisted DNA is observed; (b) for $0.01\leqslant|\sigma|\leqslant 0.043$ and forces not too large, there is significant increase in force for a given extension; (c) for $|\sigma|\geqslant 0.043$ and sufficiently large (pN) forces, abrupt jumps in extension are observed. The theory provides qualitative insight into each of these effects. For $|\sigma|<(C\omega_0)^{-1}$ there is no plectonemic supercoiling, and the chain is perturbed only slightly from the $\sigma=0$ wormlike-chain behavior; for $|\sigma|>(C\omega_0)^{-1}$ not only is the elasticity of the extended state significantly stiffer than the $\sigma=0$ case, but coexisting plectonemic supercoils further increase the force required to

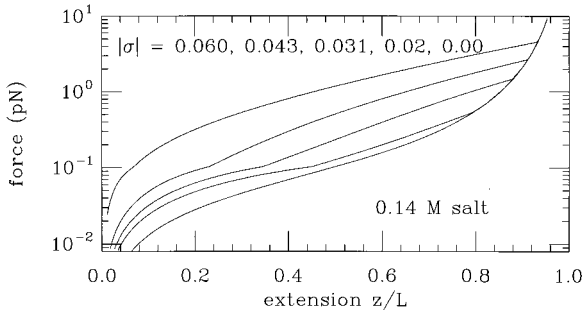

FIG. 7. Theoretical force vs extension for twisted DNA, for 0.14 M univalent salt, and with no denaturation, $A=50$ nm and $C=75$ nm. Results are shown for $|\sigma|=0$, 0.02, 0.031, 0.043, and 0.060, and are similar to those obtained for 0.01 M.

obtain a given extension. Finally, the work done extending a twisted molecule with pN forces can be $>10k_BT/\mathrm{nm}$, enough to deform the double helix. In particular, for $\sigma\approx-0.04$, a force of 1 pN is sufficient to denature DNA. The force ''plateaus'' join coexisting states of different extension in the same way that pressure plateaus join coexisting phases of three-dimensional matter with different densities.

An important experimental result is that a finite force is required to start extending the molecule for $|\sigma|$ bigger than roughly 0.04. This effect was predicted by theory on the basis that the plectonemic state, for which extension must be zero, has a much lower free energy than extended states. The plectonemic state behaves as a stable thermodynamical phase on which work must be done to convert it to extended solenoid DNA. At zero applied force, there is no extended solenoid for sufficiently large $|\sigma|$, thus the linear elasticity of the pure solenoid state of Sec. II D is hidden.

Although the theory gives a good qualitative account of the experimental data, the forces given by it in regime (b) are systematically below corresponding experimental values by roughly a factor of 2. This problem is most severe for the case $\sigma=0.01$ where theory predicts nearly the same force-distance behavior as for $\sigma=0$, while the experimental forces are significantly higher. Setting $C=100$ nm moves the $|\sigma|=0.01$ theoretical forces closer to the experimental data. On the other hand, these data are in the regime where the present theory is not precise (recall that the low-force extended solenoid free energy was constructed mainly heuristically, without a complete calculation of the large-scale conformational fluctuations; also, the calculation of the plectonemic free energy is at best accurate to $\approx k_BT/A$ due to neglect of the entropy of its bending and branching). Monte Carlo calculations are needed to study low $|\sigma|$ and low forces in more detail, and might allow C to be fit to experimental data [20].

Figure 7 shows theoretical force-distance curves for 0.14 M univalent ionic strength (the only difference from the 0.01 M case is the use of different electrostatic interactions in the plectonemic state free energy). Overall, the force-distance behavior is rather similar to that observed at 0.01 M; however, for small extensions, the forces are below the 0.01 M results, and for large extensions, the forces are above those of 0.01 M, due to the different shape of the plectonemic free energy (see Fig. 3). An increased range of plectoneme-extended coexistence at zero force occurs for 0.14 M, making the forces turn down at low extensions for $\sigma\leqslant0.06$. However, because this is controlled by the small free energy difference between the plectoneme and solenoid states for low $|\sigma|$ and low force, the theory may well be exaggerating this point.

No denaturation is included in the results for 0.14 M shown in Fig. 7. At higher ionic strength, repulsion between the phosphates along the DNA is reduced and the double helix is somewhat more stable (the helix melting temperature increases by about 10 °C for each decade increase in univalent ionic strength). However, because the screening length is reduced, the free energy of the plectoneme is lower for 0.14 M than for 0.01 M, which will tend to concentrate the linking number in the plectonemic supercoils more. These two effects act in opposite directions, making prediction of denaturation as a function of ionic strength problematic.

III. BRAIDING DNA

Consider two dsDNAs each of length L, braided together so that the linking number of either of the strands of one chain with either of the strands of the other is Ca (for ''catenation''). In this section the case where the linkages of the two strands in each dsDNA are not fixed is studied, as in experiments of Strick *et al.* where the braided DNAs were able to swivel around single-stranded attachments [7].

Since the main experimental application of this section is to the study of braided DNAs, a useful measure of catenation is as a fraction of the equilibrium linking number of dsDNA [7,10]. This ''specific catenation'' $\sigma_c=2\pi\mathrm{Ca}/(\omega_0 L)$ is a convenient dimensionless measure of catenation per length, and allows easy comparison of the properties of catenated DNAs to those of supercoiled DNAs of similar excess linkages. It must be emphasized that the use of ω_0 to normalize the catenation per length is otherwise arbitrary since DNA twisting plays no role in this section (note that the results depend only on the combination $\sigma_c\omega_0=2\pi\mathrm{Ca}/L$). Right-handed braids are assumed in this section, i.e., $\sigma_c>0$.

A. Free energy of braids without tension

1. Loose braids

If the amount of DNA per radian of braid exceeds a bending persistence length, or if $X_c\equiv\sigma_c\omega_0 A=2\pi\mathrm{Ca}A/L<1$, the DNAs will undergo random-coillike fluctuations between successive braidings. Since $A\approx50$ nm and $\omega_0\approx1.8\ \mathrm{nm}^{-1}$, this case occurs for $\sigma_c<0.01$. The braiding free energy for such ''loose braids'' may be estimated using a linear response approach similar to that used for supercoiling [6]. This begins with an estimate of the catenation squared of two closed random walks which are constrained to be near one another at one point. From the Gauss integral (1), $\langle\mathrm{Ca}^2\rangle\approx\ln[L/A]$. The wandering apart of the two chains makes this ''spontaneous catenation'' of two random walks [15] much less than the spontaneous writhe of a single random walk relevant for supercoiling [6], $\langle\mathrm{Wr}^2\rangle\approx L/A$.

The free energy for fixed $\mathrm{Ca}<L/A$ is therefore $F_c\approx\pi^2k_BT\mathrm{Ca}^2/(2\ln[L/2A])$ (the numerical factors are from the theory of wrapping of a self-avoiding chain around a line

[16]). In this regime, braiding will have little effect on the chain conformations apart from their colocalization, since there are many persistence lengths per braid (for very long DNAs some swelling of the chains will arise due to excluded-volume interactions). Therefore the chain radius will remain roughly $R_E \approx (2AL)^{1/2}$ in the loose braiding regime.

2. Tight braids

If $X_c > 1$, each radian of braid contains less than a persistence length, and well-defined braids will occur with each chain forming a superhelix of average radius R and pitch P [Fig. 2(b)]. For the moment it is assumed that that the braid axis has no appreciable writhe, so the catenation number is $\mathrm{Ca} = L/(2\pi\ell)$, where $\ell^2 = R^2 + P^2$. Thus the topological constraint sets $\ell = 1/(\sigma_c \omega_0) = A/X_c$.

The catenation free energy per length, for $\sigma_c \omega_0 A > 1$, is Eq. (8) without the twist energy term

$$\frac{\mathcal{F}_c(\sigma_c)}{k_B T} = \min_R \left[\frac{A}{2} (\sigma_c \omega_0)^4 R^2 + A^{-1/3} R^{-2/3} + A^{-1/3} (\pi P)^{-2/3} + w(R) + w(\pi P) \right]. \tag{21}$$

The first term is the average bending energy, the second and third are the entropy cost of confinement of the DNA in a braid. The final terms are direct electrostatic interactions of the two DNAs in the braid, important when R or πP become comparable with the screening length λ_D. Minimization of Eq. (21) determines R.

To understand the scaling behavior of Eq. (21), consider only the bending and entropic repulsion terms dependent on R,

$$\mathcal{F}_c(\sigma_c) A / k_B T \approx X_c^4 (R/A)^2/2 + (A/R)^{2/3}, \tag{22}$$

which has its minimum at $R = (2/3)^{3/8} A / X_c^{3/2}$ as the braid is tightened, its radius is reduced. The free energy per length is $\mathcal{F}_c / k_B T = 2(2/3)^{3/4} X_c / A = 4\pi (2/3)^{3/4} \mathrm{Ca}/L$: each radian of braid introduces one more constraint into the polymer conformation, and costs on the order of a $k_B T$. The free energy per length becomes on the order of $k_B T/A$ for $X_c \approx 1$, near to the edge of the tight braiding regime. Finally, the correlation length for the fluctuations of the chain inside the braid is $\xi \approx A^{1/3} R^{2/3} \approx A/X_c = 1/(\sigma_c \omega_0)$, just the length of DNA in a radian of braid, the same as for plectonemic supercoiled DNA [6].

Figure 8 shows the free energy of the straight braid, as a function of σ_c, for $A = 50$ nm and for 0.01 and 0.14 M univalent salt, obtained from minimization of Eq. (21) with respect to R. For 0.01 M, the free energy rises linearly with σ_c until about $\sigma_c = 0.03$, after which the electrostatic interactions begin to dominate, and the free energy rises quadratically with σ_c. For 0.14 M, the shorter screening length delays the upturn in the free energy from its initial linear rise to about $\sigma_c = 0.06$. The catenation free energy is very similar to the free energy for a plectonemically supercoiled DNA (Fig. 3). Figure 9 shows the straight braid radius and pitch for the

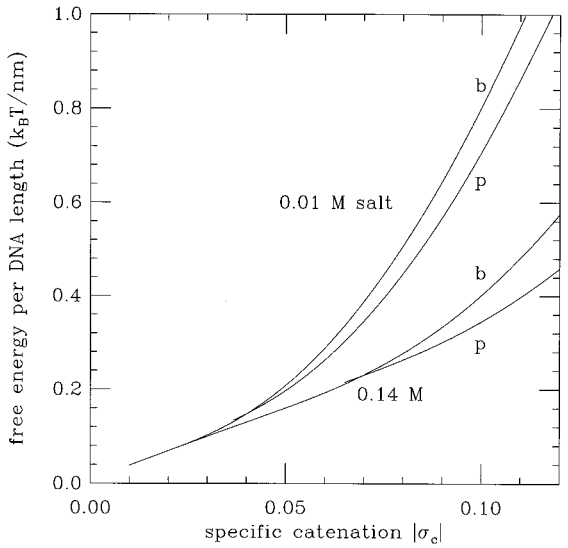

FIG. 8. Free energy per length of DNA, for two dsDNAs braided with specific catenation of σ_c, in the tight braiding regime. Results are shown for 0.01 M and 0.14 M univalent salt, and for $A = 50$ nm. The curves labeled ''b'' show the result for unsupercoiled (straight) braids, while those labeled ''p'' show the result for plectonemically supercoiled braids.

0.14 M case; these start out on the order of a persistence length for $\sigma_c \approx 0.01$, and drop to a few nanometers when $\sigma_c \approx 0.05$.

The slope of the tight braid catenation free energy shown in Fig. 8 is proportional to the work done on the straight braid with σ_c, per unit increase in Ca. The free energy change of the braided DNAs per added catenation (Fig. 10) is

$$\frac{dF_c}{d\mathrm{Ca}} = \frac{d(2L\mathcal{F}_c)}{d\mathrm{Ca}} = \frac{4\pi}{\omega_0} \frac{d\mathcal{F}_c}{d\sigma_c}. \tag{23}$$

At the beginning of the regime where Eq. (21) is reasonable, $X_c \approx 1$ or $\sigma_c \approx 0.01$, this is already $20 k_B T$ per braid [the result obtained from Eq. (22) is $8\pi(2/3)^{3/4} k_B T$] and then further increases as the electrostatic interactions start to force the free energy to increase quadratically for σ_c bigger than about 0.05.

There is a slight nonconvexity in the braid free energy of Fig. 8, and a corresponding region of slight negative slope in Fig. 10. This arises from the linearity in σ_c of the scaling part of the free energy, leaving convexity to be determined by correction terms: it turns out that for Eq. (21) the free energy is slightly nonconvex. This is a weak effect which is easily overwhelmed by slight changes to the form of Eq. (21). But, if this nonconvexity survives, it will lead to ''phase separation'' of the braiding into regions characterized by different σ_c.

3. Phase separation of tight and loose braids

A more robust braid phase separation phenomenon is implied by comparison of the tight and loose braid free energies. The free energy per added catenation in the tight braid regime (23) is less than the free energy per added

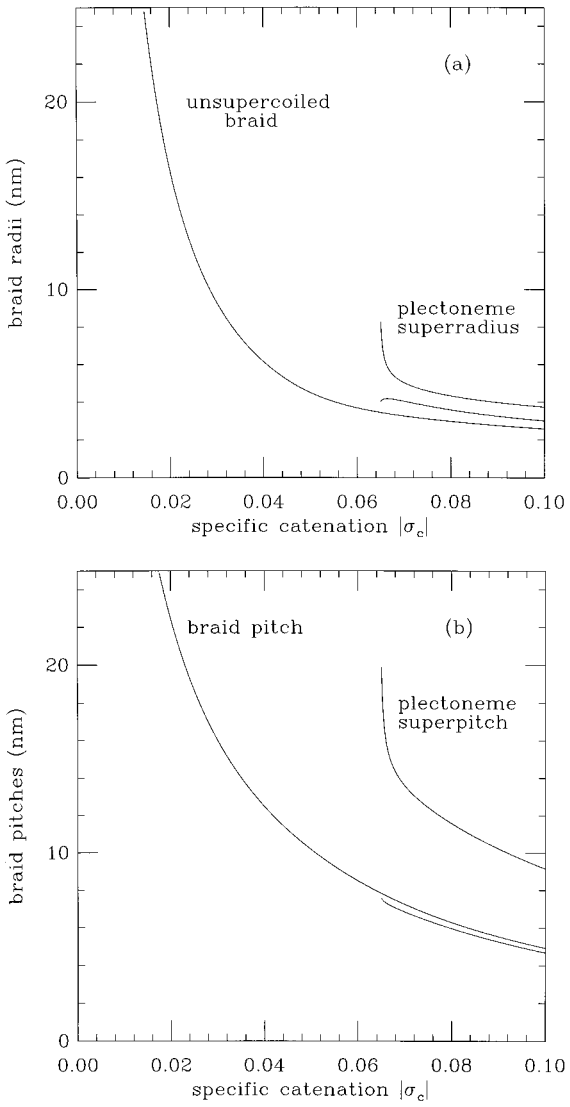

FIG. 9. Geometry of braided DNAs, for 0.14 M univalent salt, and $A=50$ nm. Radii (a) and pitches (b) are shown as a function of σ_c. For $\sigma_c<0.06$, the unsupercoiled (straight) braid is stable, while for σ_c larger than about 0.06, plectonemically supercoiled braids are stable. The braid radius and pitch (curves starting at $\sigma_c\approx 0.06$, near to unsupercoiled radius and pitch curves) change by only a small amount when the braid supercoils. The superradius and superpitch (upper curves for $\sigma_c>0.06$) are larger than the braid radius and pitch.

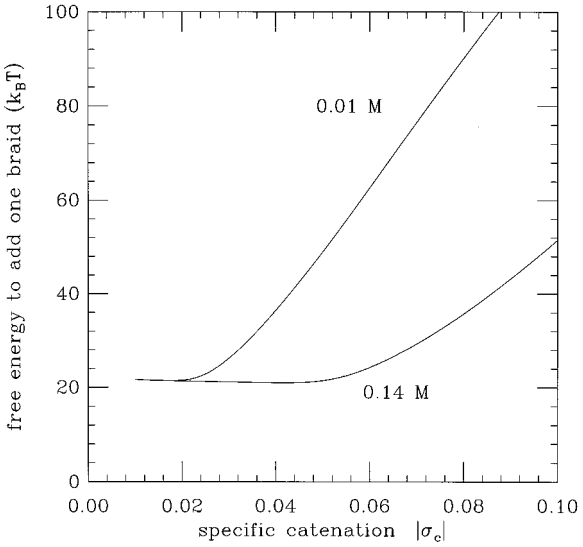

FIG. 10. Free energy to add one more braid to two DNAs with specific catenation σ_c, in the tight braiding regime. Results are shown for 0.01 and 0.14 M univalent salt, for $A=50$ nm. Addition of a braid requires more than 20 k_BT for $|\sigma_c|\geqslant 0.01$.

catenation of loose braids, $dF_c/d\mathrm{Ca}\approx\pi^2 k_BT\mathrm{Ca}/\ln[L/2A]$, for $\mathrm{Ca}>(8/\pi)(2/3)^{3/4}\ln[L/2A]\approx 2\ln[L/2A]$. In this regime, addition of loose braids is energetically unfavorable, and instead, added braids will be tight. Therefore for large L/A, in the range $L/A>\mathrm{Ca}>\ln[L/A]$ phase separation of tight and loose braids should occur. In contrast to the case of phase coexistence of supercoiled states mentioned in Sec. II C, the $\ln L$ dependence of the loose-braid free energy permits macroscopic braid phase separation.

Braid phase separation will cause the free energy per added braid of Fig. 10 to take on a nearly constant value $\approx 20k_BT$ down to low values of $\sigma_c\approx(2\pi/\omega_0 L)\ln[L/2A]$. This surprising possibility needs further exploration with computer simulation of braided chains. Experimentally, coexistence of tightly and loosely braided domains at low σ_c might be observed using fluorescence microscopy.

4. Supercoiling of a braid

At what value of σ_c will braided DNAs supercoil? A well-defined braid ($X_c>1$) may be roughly considered to be a double-helix polymer with persistence length of roughly $A_{\mathrm{eff}}=2A$, since it is made up of two intertwined chains each with persistence length A. The effective twisting persistence length is $C_{\mathrm{eff}}=\partial^2\mathcal{F}_c(\sigma_c)/\partial(\sigma_c\omega_0)^2$, which is *zero* for the scaling solution discussed above. So, braids with $X_c>1$ have an effective bending modulus higher than that of dsDNA, and an effective twisting modulus lower than that of dsDNA. This suggests that supercoiling is less favorable for braids than for dsDNA—there is less twist energy to relax by writhing.

To address this in more detail, consider a helical braid of pitch P and radius R, wrapped into a superhelix of superpitch $\mathcal{P}$ and superradius $\mathcal{R}$; define $\ell^2=R^2+P^2$ and $\mathcal{L}^2=\mathcal{R}^2+\mathcal{P}^2$. The tangent vectors $\mathbf{t}_\pm$ of the two braided DNAs in space-fixed coordinates can be constructed by composing two rotations

$$\mathbf{t}_\pm=\begin{bmatrix}\cos\frac{Ps}{\ell\mathcal{L}} & -\sin\frac{Ps}{\ell\mathcal{L}} & 0\\ \sin\frac{Ps}{\ell\mathcal{L}} & \cos\frac{Ps}{\ell\mathcal{L}} & 0\\ 0 & 0 & 1\end{bmatrix}\left(\frac{P}{\ell}\begin{bmatrix}0\\ \mathcal{R}/\mathcal{L}\\ \mathcal{P}/\mathcal{L}\end{bmatrix}\pm\frac{R}{\ell}\cos(s/\ell)\begin{bmatrix}1\\0\\0\end{bmatrix}\right.$$
$$\left.\mp\frac{R}{\ell}\sin(s/\ell)\begin{bmatrix}0\\ -\mathcal{P}/\mathcal{L}\\ \mathcal{R}/\mathcal{L}\end{bmatrix}\right). \tag{24}$$

The column vectors on the RHS are the tangent, normal, and

binormal vectors for the superhelix, in cylindrical coordinates $\{r,\theta,z\}$. The braiding of the DNAs is generated by right-handed rotation of the DNA tangent vector (chosen to make a superhelix opening angle $\gamma=\sin^{-1}P/\ell$) around the superhelix one turn every $2\pi\ell$ change in s. Space-fixed coordinates are obtained by rotating the cylindrical coordinates one turn for each $2\pi\mathcal{L}\ell/P$ change in s. Here, $\mathcal{P}$ is signed: $\mathcal{P}>0$ generates a right-handed superhelix, $\mathcal{P}<0$ generates a left-handed one.

The tangent to the curve traced by the midpoint between points at the same s on the two helicies is $\mathbf{t}=(\ell/P)(\mathbf{t}_+ + \mathbf{t}_-)/2$; the factor of ℓ/P normalizes the midpoint tangent, making up for the length ''stored'' in the helical braid. Integration of $\mathbf{t}$ verifies that this midpoint follows a superhelix of pitch $\mathcal{P}$ and radius $\mathcal{R}$.

The curvature squared of the superhelical braids may be computed, and averaged over s to yield

$$\overline{\left(\frac{d\mathbf{t}_\pm}{ds}\right)^2}=\frac{P^4}{\ell^4}\frac{\mathcal{R}^2}{\mathcal{L}^4}+\frac{R^2}{\ell^4}\left(1+\frac{\mathcal{P}P}{\mathcal{L}^2}\right)^2+\frac{R^2P^2\mathcal{R}^2}{2\ell^4\mathcal{L}^4}. \quad (25)$$

There were s-dependent (oscillating) terms in the curvature before averaging, as Eq. (24) is not a stationary state of elasticity theory. Consider a few special cases. If the braid radius $R=0$, the two tangents $\mathbf{t}_\pm$ reduce to the superhelix tangent $\mathbf{t}$, and Eq. (25) becomes $\mathcal{R}^2/\mathcal{L}^4$. If $\mathcal{R}=\infty$, there is no curvature of the superhelix, and Eq. (25) becomes just the curvature squared of the braid, R^2/ℓ^4. If $\mathcal{R}=0$, the superhelix degenerates to the z axis, and Eq. (25) becomes $(1+P/\mathcal{P})^2R^2/\ell^4$. In this case, the superhelix acts to change the rate of rotation of the braid: note that if $\mathcal{P}=-P$, the curvature vanishes, as the two tangents become just $\mathbf{t}_\pm(s)=\mathbf{z}$. In general, this effect of unwinding of the braid by the superhelix results in a reduction of the curvature energy if the sign of $\mathcal{P}$ is set opposite to that of P, relative to the case where the two helicies have the same handedness.

The catenation number of the superhelical braid may be computed using the fact that it is invariant under deformation of the two braided curves onto the midpoint superhelix (assuming that no ''accidental'' crossings of the braids occur during this process). One such deformation is obtained by taking $R\to 0$. This deformation gives the familiar ribbon model of a superhelical DNA with constant radius $\mathcal{R}$ and pitch $\mathcal{P}$, and of total length LP/ℓ. The ribbon twist per length of superhelix is $2\pi\mathrm{Tw}/(LP/\ell)=1/P+\mathcal{P}/\mathcal{L}^2$, the sum of the one radian every distance P along the superhelix that the ribbon director turns around the superhelix bending normal vector, and the superhelix torsion [19].

The ribbon writhe per length of superhelix is $2\pi\mathrm{Wr}/(LP/\ell)=-\mathcal{P}/\mathcal{L}^2$ for plectonemic supercoiling. The total catenation number of the braid is the sum of the total twist and writhe, $2\pi\mathrm{Ca}/L=\sigma_c\omega_0=1/\ell$ for the plectoneme (for solenoidal supercoiling, the corresponding result is $\sigma_c\omega_0=[1+\mathrm{sign}(\mathcal{P})P/\mathcal{L}]/\ell$).

The free energy per length of DNA for a supercoiled braid is

$$\frac{\mathcal{F}_{c,p}(\sigma_c)}{k_BT}=\min_{R,\mathcal{R},\mathcal{P}}\left\{\frac{A}{2\ell^4}\left[\left(1+\frac{\mathcal{P}P}{\mathcal{L}^2}\right)^2R^2+\frac{P^4\mathcal{R}^2}{\mathcal{L}^4}+\frac{P^2R^2\mathcal{R}^2}{2\mathcal{L}^4}\right]\right.$$
$$+\frac{1}{A^{1/3}R^{2/3}}+w(R)+\frac{1}{2(2A)^{1/3}\mathcal{R}^{2/3}}+2w(\mathcal{R})$$
$$+\frac{1}{A^{1/3}(\pi P)^{2/3}}+w(\pi P)+\frac{1}{2(2A)^{1/3}(\pi\mathcal{P})^{2/3}}$$
$$\left.+2w(\pi\mathcal{P})\right\}. \quad (26)$$

These terms account for the bending energy from Eq. (25), the free energy cost of confining DNA in a braid of radius R, direct interactions across the braid of radius R, the free energy cost of confining the braid to a superhelix of radius $\mathcal{R}$ ($2A$ is taken as the braid persistence length; the additional 1/2 comes from the fact that the free energy is per length of DNA which is $2L$ for the braid), and additional direct interactions across the superhelix of radius $\mathcal{R}$. The final terms account for entropic and direct interactions in the case that the pitches become small.

The free energy (26) reduces to the unsupercoiled braid free energy (21) for $\mathcal{R},\mathcal{P}\to\infty$. For small enough X_c the unsupercoiled braid state is recovered, while for large X_c, supercoiled states become stable. Numerical minimization of Eq. (26) gives the plectonemic state free energies shown in Fig. 8, for 0.01 M and 0.14 M salt. The stable plectonemes all have opposite superhelix and braid helix handedness.

For 0.14 M, there is no plectonemic minimum until $\sigma_c\approx 0.06$; the free energy of the plectoneme does not drop below that of the straight braid until $\sigma_c\approx 0.07$. At 0.01 M, the plectoneme state appears at about $\sigma_c=0.04$ and becomes lower in free energy than the straight braid at $\sigma_c\approx 0.045$. The plectoneme braid is stabilized relative to the straight braid by stronger electrostatic interactions (which impart additional effective twist rigidity to the braid, Fig. 8). Figure 9 includes the superradius and superpitch for the 0.14 M plectonemic state; the superradius is slightly larger than the braid radius (the supercoiled braids thus do not interpenetrate) and the superpitch stays reasonably large compared to the braid pitch (this is also true for the 0.01 M state). When the plectoneme forms, the braid radius and pitch are only slightly shifted from their straight-braid values.

The main difference of this model from that for supercoiled DNA is that the braid has peculiar effective twisting elasticity. In the theory of supercoiling of DNA, the harmonic twist elasticity plays an essential role: writhing is driven so as to reduce the DNA twist. In the supercoiled braid, the twistlike energy is subharmonic in form, and writhing is thus not strongly driven (note that the supercoiled braid free energies are only slightly lower than those for the straight braids). The bending energy term which drives the writhing of the braid is the first one in Eq. (26), which accounts for the interaction of the chirality of the braid and of the superhelix: opposite chiralities of the braid and superhelix tend to reduce the bending energy by ''untwisting'' the braid. This term is roughly analogous to the twist energy for supercoiled DNA.

5. Toroidal catenanes

Imagine closing two braided DNAs to obtain a toroidal link of two circular DNAs. Such toroidal links (''catenanes'') of DNA molecules are produced in cells when circular DNAs are duplicated [11]. The preceding theory for braid supercoiling should apply to catenanes. In fact, plectonemic supercoiling has been observed in Monte Carlo (MC) simulations of catenanes [10]. Most of the simulations were for a hard-core interaction that corresponded to 0.01 M NaCl, and plectonemic configurations were observed only for $|\sigma_c|>0.05$ (see Fig. 6 and p. 1138 of Ref. [10]), in agreement with the calculations of the preceding section.

Electron microscopy of 3.5 kb plasmids has been done [11] for Ca$\leqslant$18, or for $\sigma_c\leqslant 0.054$. The plasmids were ''nicked'' so that the double-helix linkages were allowed to freely fluctuate. Although the braid axis collapses onto itself as Ca is increased (see Fig. 3 of Ref. [11]), plectonemic supercoiling was not obvious. Higher Ca should be studied (Ca$>$20), since both theory and simulation indicate that $\sigma_c>0.05$ is the regime where braid supercoiling occurs.

B. Force-distance behavior of a braid

1. Loose braids ($X_c<1$)

For low forces ($f<k_BT/A$) one expects linear polymer elasticity, $f\propto z$, ignoring excluded volume effects. For $X_c=0$ there are two independent chains, and the force versus distance should be just that of two DNAs in parallel, or $f\approx(3k_BT/A)z/L$. For larger $X_c>0$ but still $X_c<1$, it was argued that the chain conformations should not be strongly perturbed from random coils over most of their length, and thus little change in the elasticity will occur as X_c is increased.

The situation can be made slightly more precise for large forces: since the mean interbraid distance $1/(\sigma_c\omega_0)$ is larger than the persistence length, for high forces ($f>k_BT/A$) which establish a thermal correlation length smaller than A [19], the elasticity will be essentially unaffected by the braiding. Thus the elasticity for $f>k_BT/A$ will again reduce to that of two DNAs in parallel. In summary, for two loosely braided DNAs each of length L, a reasonable estimate of the force required to obtain extension z is just [19]

$$f=\frac{2k_BT}{A}\left[\frac{z}{L}+\frac{1}{4(1-z/L)^2}-\frac{1}{4}\right]. \tag{27}$$

2. Tight braids ($X_c>1$)

In this regime the force needed to achieve a given extension z increases with increasing X_c. If there is no supercoiling (low enough X_c), then for low forces $f<k_BT/A$, linear elasticity of the general form $f\approx(k_BT/A)z/L$ should be observed; the prefactor should slowly rise with X_c.

If the braid is fully supercoiled at zero tension ($\sigma_c>0.05$), no extension will occur below a threshold force, reflecting the fact that some work must be done to convert the supercoiled braid into an extended braid. The extension should rapidly increase with force as the supercoiled braid is converted to an extended braid in a fashion similar to the conversion of supercoiled DNA to extended DNA computed above.

Once the braid is straightened, one must worry about its stretching. For high enough forces, the correlation length for ordinary dsDNA under tension, $\xi=(k_BTA/f)^{1/2}$, will be smaller than the length of DNA in a braid, A/X_c (which is also the thermal correlation length for fluctuations in the braid under zero tension). Thus the elasticity of the braid will reduce to that of two DNAs in parallel, Eq. (27), for $f>X_c^2k_BT/A$.

This conclusion can be obtained from a more detailed calculation of the stretching of the DNA in a straightened-out braid, where $R\ll P$ and the fluctuations are small. The free energy of the braid in the fluctuating-length ensemble is Eq. (21) minus $(f/2)(z/L)$ (the 2 accounts for the sharing of the tension by the two braided chains). The extension fraction z/L is reduced by two effects: first, the helix structure of the braid reduces z/L by a factor P/ℓ. A further reduction of length arises from thermal fluctuations. This second, thermal length reduction may be estimated from the average orientation of a chain confined to a tube of radius R, which is $1-(R/A)^{2/3}/4$ (the mean angle the chain makes with the tube is $\sim R/\xi$, where the correlation length $\xi\sim A^{1/3}R^{2/3}$ is that of a wormlike chain confined in a tube [6]; the orientation is the cosine of that angle). The free energy at fixed force is therefore

$$\frac{\mathcal{G}_{c,s}(\sigma_c,f)}{k_BT}=\min_R\left[\frac{A}{2}(\sigma_c\omega_0)^4R^2+A^{-1/3}R^{-2/3}-\frac{f}{2}\frac{P}{\ell}\left(1-\frac{R^{2/3}}{4A^{2/3}}\right)\right]. \tag{28}$$

For large forces the behavior of Eq. (28) is revealed by setting $P/\ell=1-R^2/(2\ell^2)$ (R/ℓ will be driven to zero in that limit). The dominant terms are $\mathcal{G}_c/k_BT=A^{-1/3}R^{-2/3}+(f/8)R^{2/3}A^{-2/3}$ which is minimized for $R=A^{1/4}(f/8)^{-3/4}$. So, $z/L=1-(2fA)^{-1/2}$, the extension of a DNA under tension $f/2$. This holds as long as the leading bending energy term of Eq. (28) is negligible, or for $f>X_c^2k_BT/A$ as argued above. Braiding thus establishes a tension of $X_c^2k_BT/A$.

IV. DISCUSSION

This paper has discussed the elasticity of polymers subject to topological constraint. Most of what has been presented either has been, or can be studied experimentally. Section II discussed the problem of the elasticity of dsDNA where the linking number of the two strands was held fixed. If Lk is near the equilibrium value of one link per 10.5 bp, the elasticity reduces to that of a wormlike chain, and is characterized by the force $k_BT/A\approx 0.08$ pN. For small changes of Lk from this value, there is little change in the elasticity; to perturb the polymer elasticity, $|\mathrm{Lk}-\mathrm{Lk}_0|$ must exceed roughly one link for each twisting persistence length $C\approx 75$ nm (about 220 bp) along the molecule; this corresponds to a specific linking change of about $|\sigma|>0.01$. For larger linkage change, the force needed to obtain a given extension is increased significantly over most of the extension range. For $|\sigma|>0.03$, plectonemic supercoils are stable at low forces, and once the entire polymer is bound to itself as a plectonemic supercoil, a finite force should be required to achieve

any extension at all. For sufficiently large $|\sigma|$ and force, enough work is done on the DNA that one can expect the double helix to undergo abrupt structural transitions.

These effects were predicted [6] and recently have been experimentally observed [7]. Section II emphasizes that the analytical theory gives a good account of these experiments. The elastic parameters were not fit (the values $A=50$ nm and $C=75$ nm are taken from previous experiments), and theory and experiment agree well in the regime where the elasticity is primarily entropic.

Experimental data for force ''plateaus'' allows the denaturation parameters σ_d and σ_D to be fit for over- and undertwisted DNA. The free energy of the new DNA states is roughly 15 k_BT/nm above the free energy of the unperturbed double helix, reasonable since it is known that the free energy of the double helix is on the order of 10 k_BT/nm lower than separated single strands. The crude model used here supposes that denaturation occurs in plectonemelike ''bubbles'' which do not contribute to the total chain extension; both the number of parameters and the complexity of the calculation are reduced by this assumption. A more general model might allow a better description of some aspects of the experimental data (e.g., the shift in extension away from the $\sigma=0$ curve above the denaturation plateau), and unify the denaturation of twisted DNA with the overstretching transition observed at high forces for $\sigma=0$ [8,9]. An immediately obvious feature of an extensible wormlike-chain model of DNA is that stretching will be linearly coupled to twist; this is a consequence of chirality of the double helix, which eliminates twist reversal as a symmetry [14]. A consequence of this coupling is that external stresses on a chain (e.g., hydrodynamic drag) can couple to the twist degrees of freedom of DNA in a solution, indicating that twisting and writhing may play a role during stress relaxation in solutions of twist-storing polymers.

Strick *et al.* have also braided two DNAs around one another [7]. In this case, the catenation number Ca of the two double helicies with each other is constrained. For small enough Ca, the free energy of addition of one braid is small compared to k_BT. However, for more than one braid per persistence length, or for $|\sigma_c|>0.01$, each successive braid costs a free energy of about 20 k_BT. This holds until the braid is so tight that direct electrostatic repulsion between the two DNAs starts to drive the free energy to increase even more quickly (for roughly $|\sigma_c|>0.05$). At this point, it starts to become favorable for the braid itself to supercoil. Braids will thus have force-distance behavior reminiscent of that of supercoiled DNA. A final intriguing feature of sufficiently long braided DNAs is that for $\ln[L/A]<\mathrm{Ca}<L/A$, there will be ''phase separation'' of the braids into domains of tight and loose braiding.

The braid results should also apply to braids of polymers other than DNA, to high-order catenanes of two DNAs, and to toroidal knots of high order (obtained by linking the ends of a single plectonemically supercoiled loop). The techniques of this paper might be applied more generally to knots, if one can find a relation between knot topology and average interstrand distance. Knotted DNAs are generated by site-specific recombination enzymes [22], and their conformational statistics are not well understood.

Biological relevance

The braiding free energy is relevant to an important biological problem, the initial stages of separation of replicated DNAs. Replication of a long DNA occurs by separation of the two complementary single ''parent'' strands, each of which acts as a template for synthesis of new strands. The enzymatic machinery that accomplishes this feat is located near the seperatrix between the parent strands, the ''replication fork,'' and moves progressively down the molecule. The size of regions of DNA that are replicated by one fork (''replication units'') are about 10^4 bp, and are much larger than the replication machinery.

The parent strands, originating as dsDNA, are catenated once every 10.5 bp. For the replicated molecules to be physically separated (they are bound for different cells in the case of chromosomal DNAs) *every one* of these catenations must be removed [12]. Before replication, the parent DNA can be untwisted upstream of the fork by enzymes (in the bacterium *E. coli*, the enzyme gyrase is believed to do this). Such enzymes act locally, and can greatly reduce the linkage of the parents, but they cannot be expected to be able to sense when the linkage is exactly zero: the daughter DNAs will end up braided [12].

Remnant catenations of the replicated daughter DNAs must be removed by the passage of one daughter DNA through the other, by the action of a type II topoisomerase enzyme (in *E. coli*, these are gyrase, and topoisomerase IV). Once again, since these enzymes act locally, they cannot sense when the catenation has been reduced to precisely zero. A locally acting decatenation process can at best systematically reduce Ca to the level where k_BT of free energy is liberated per double strand passage event. Below this level of catenation, thermal fluctuations generate as much stress in the DNA as the catenation, and Ca will fluctuate thermally.

In Sec. III it was found that adding more than one braid per persistence length costs appreciably more than a k_BT per braid. It is therefore reasonable to suppose that this free energy gain can guide topoisomerases to relax the catenation of two DNAs to the lower edge of the tight braid regime, or to $\mathrm{Ca}\approx L/A$. Relaxation to lower Ca values (i.e., into the regime where tight and loose braids coexist) requires equilibration of the DNAs on length scales much larger than a persistence length, and can be expected to occur sluggishly, or not at all. Therefore, in the absence of other mechanisms for decatenation, topoisomerases acting on duplicate sister DNAs will leave one braid every few hundred bp (on the order of hundreds per replication unit).

This could be directly studied in an experiment on braided DNAs similar to that of Strick *et al.*; [7] but with topoisomerase II present. The decatenation rate for topo II at a given concentration will drop to zero for $|\mathrm{Ca}|<L/A$ or for $|\sigma_c|<0.01$; below this level Ca will ''diffuse'' rather than decreasing systematically with time.

How is Ca systematically reduced to precisely zero? In prokaryote cells, DNA plasmids (circles of 1 kb to 100 kb) are believed to be decatenated by ''decatenase'' enzymes. Bacteria deficient in these enzymes duplicate plasmids, but are unable to decatenate them: in the electron microscope one observes catenated plasmids with roughly one right-handed catenation per DNA persistence length [12,23], in agreement with the arguments described above (remark-

ably, no systematic study has been done of the number of catenations left in plasmids as a function of plasmid size).

How can decatenases work? The following scheme has been suggested by Zechiedrich and Cozzarelli [12]; the results of this paper indicate how thermodynamics can play a role in it. Consider two dsDNAs with positive catenation $\sigma_c < 0.01$: no locally acting decatenase can effectively separate them. However, imagine that the circles are now negatively supercoiled (e.g., by the action of gyrase, which drives σ to high negative values using energy from ATP hydrolysis). Supercoiling will increase the stress acting *between* the two catenated molecules (the relevant free energy is that of a toroidal catenane with fixed Ca *and* fixed double-helix Lk's and can be estimated by means similar to those used in this paper). This stress will guide decatenase to remove both Ca and Lk, since a locally acting decatenase will be unable to distinguish between inter- and intramolecule strand passages; however, the continued action of gyrase will replenish Lk and *not* Ca. The end effect is a systematic reduction of Ca to zero, accompanied by negative supercoiling of the two plasmids. Note that supercoiling-induced crowding will also thermodynamically drive the removal of mutual and self-knots of the chains.

In addition to explaining how decatenase could work, this suggests why plasmids are generally negatively supercoiled, and implies that the efficiency of decatenation will drop if gyrase alone is inhibited [12]. A similar process could be used in the early stages of separation of bacterial chromosomes (10^6 BP), which are organized into a succession of supercoiled ''loop'' domains.

There remains the problem of the separation of huge linear chromosomal DNAs (up to 10^9 bp) in eukaryotic cells. Eukaryote chromosomes are made up of ''chromatin fibre,'' consisting of DNA wrapped around protein complexes called nucleosomes. There is one nucleosome every 200 bp, and in the electron microscope the resulting fiber looks like a long bead necklace. Chromatin fiber has a persistence length of roughly 50 nm, containing about 1 kb of DNA (recall that ''bare'' DNA has a persistence length of 150 bp) [24]. The arguments of Sec. III indicate that topo II will reduce the catenation of chromatin fibres (the nucleosomes are added onto bare patches of DNA slightly downstream of the replication fork [25]) to below $\sigma_c = 0.001$. However, for a 10^8 bp chromosome, this leaves $\mathrm{Ca} \approx 10^4$.

If the number of bp per persistence length of chromatin were systematically increased, the results of Sec. III indicate that topo II would in turn systematically remove this remanant Ca. In fact, following DNA replication, eukaryote chromosomes *condense* along their length and become visible first as long, apparently flexible strings, which then become rather inflexible fat sausages. Condensation causes gradual stiffening and shortening of the chromosomes, both effects plausibly favoring the removal of catenations, and other entanglements. The same phenomena might be studied in the test tube if one could monitor the level of entanglement of DNAs as a function of persistence length which might be altered using DNA-binding proteins or by adjusting ionic conditions.

ACKNOWLEDGMENTS

The author thanks D. Bensimon, N. R. Cozzarelli, V. Croquette, M. Schmid, T. Strick, E. D. Siggia, A. Stasiak, and A. V. Vologodskii for helpful discussions. This research was supported by the Meyer Foundation.

[1] P. J. Hagerman, Annu. Rev. Biophys. Biophys. Chem. **17**, 265 (1988).

[2] W. H. Taylor and P. J. Hagerman, J. Mol. Biol. **212**, 363 (1990).

[3] D. M. Crothers, J. Drak, J. D. Kahn, and S. D. Levene, Meth. Enzymology **212**, 3 (1992).

[4] S. B. Smith, L. Finzi, and C. Bustamante, Science **258**, 1122 (1992); C. Bustamante, J. F. Marko, E. D. Siggia, and S. Smith, Science **265**, 1599 (1994).

[5] T. T. Perkins, S. R. Quake, D. E. Smith, and S. Chu, Science **264**, 822 (1994); T. T. Perkins, D. E. Smith, R. G. Larson, and S. Chu, Science **268**, 83 (1995).

[6] J. F. Marko and E. D. Siggia, Science **265**, 506 (1994); Phys. Rev. E **52**, 2912 (1995).

[7] T. R. Strick, J.-F. Allemand, D. Bensimon, A. Bensimon, and V. Croquette, Science **271**, 1835 (1996).

[8] P. Cluzel, A. Lebrun, C. Heller, R. Lavery, J.-L. Viovy, D. Chatenay, and F. Caron, Science **271**, 792 (1996).

[9] S. B. Smith, Y. Cui, and C. Bustamante, Science **271**, 795 (1996).

[10] A. V. Vologodskii and N. R. Cozzarelli, J. Mol. Biol. **232**, 1130 (1993).

[11] S. D. Levene, C. Donahue, T. C. Boles, and N. R. Cozzarelli, Biophys. J. **69**, 1036 (1995).

[12] E. L. Zechiedrich and N. R. Cozzarelli, Genes Devel. **9**, 2859 (1995).

[13] F. B. Fuller, Proc. Natl. Acad. Sci. USA **75**, 3557 (1978); see, also, M. D. Frank-Kamenetskii and A. V. Vologodskii, Usp. Fiz. Nauk **134**, 641 (1981) [Sov. Phys. Usp. **24**, 679 (1982)]; N. R. Cozzarelli, T. C. Boles, and J. White, in *DNA Topology and its Biological Effects*, edited by N. R. Cozzarelli and J. C. Wang (Cold Spring Harbor Laboratory, Cold Spring Harbor, NY, 1990), Chap. 4; A. V. Vologodskii and N. R. Cozzarelli, Annu. Rev. Biophys. Biomol. Struct. **23**, 609 (1994).

[14] J. F. Marko and E. D. Siggia, Macromolecules **27**, 981 (1994); Macromolecules **29**, 4820 (1996).

[15] S. Prager and H. L. Frisch, J. Chem. Phys. **46**, 1475 (1967); S. F. Edwards, Proc. Phys. Soc. London **91**, 513 (1967); S. F. Edwards and J. W. Kerr, J. Phys. C **5**, 2289 (1972); N. Saito and Y.-d. Chen, J. Chem. Phys. **59**, 3701 (1973); H. Kleinert, *Path Integrals in Quantum Mechanics, Statistics and Polymer Physics* (World Scientific, Teaneck, NJ, 1990), Sec. 16.1.

[16] J. Rudnick and Y. Hu, Phys. Rev. Lett. **60**, 712 (1988).

[17] D. Stigter, Biopolymers **16**, 1435 (1977); A. Vologodskii and N. Cozzarelli, *ibid.* **35**, 289 (1995).

[18] T. C. Boles, J. H. White, and N. R. Cozzarelli, J. Mol. Biol. **213**, 931 (1990).

[19] J. F. Marko and E. D. Siggia, Macromolecules **28**, 8759 (1995).
[20] A. V. Vologodskii and J. F. Marko (unpublished).
[21] A. V. Vologodskii, *Topology and Physics of Circular DNA* (CRC, Boca Raton, FL, 1990), Chap. 4.
[22] S. J. Spengler, A. Stasiak, and N. R. Cozzarelli, Cell **42**, 325 (1985); J. B. Bliska and N. R. Cozzarelli, J. Mol. Biol. **194**, 205 (1987); S. A. Wasserman and N. R. Cozzarelli, J. Biol. Chem. **266**, 20567 (1991); N. J. Crisona, R. Kanaar, T. N. Gonzalez, E. L. Zechiedrich, A. Klippel, and N. R. Cozzarelli, J. Mol. Biol. **243**, 437 (1994).
[23] D. E. Adams, E. M. Shekhtman, E. L. Zechiedrich, M. B. Schmidt, and N. R. Cozzarelli, Cell **71**, 277 (1992).
[24] C. Castro, Ph.D. thesis, University of Oregon, 1994.
[25] A. Wolffe, *Chromatin* (Academic, San Diego, CA, 1995), Chap. 2.